



ChemR23 signaling ameliorates cognitive impairments in diabetic mice via dampening oxidative stress and NLRP3 inflammasome activation

Jiawei Zhang^{a,1}, Lan Liu^{a,1}, Yaxuan Zhang^a, Yuan Yuan^a, Zhijuan Miao^a, Kaili Lu^a, Xiaojie Zhang^a, Ruiqing Ni^{b,c}, Haibing Zhang^d, Yuwu Zhao^{a,**}, Xiuzhe Wang^{a,*}

^a Department of Neurology, Shanghai Sixth People's Hospital Affiliated to Shanghai Jiao Tong University School of Medicine, Shanghai, China

^b Institute for Regenerative Medicine, University of Zurich, Zurich, Switzerland

^c Institute for Biomedical Engineering, ETH Zurich, Zurich, Switzerland

^d CAS Key Laboratory of Nutrition, Metabolism and Food Safety, Shanghai Institute of Nutrition and Health, University of Chinese Academy of Sciences, Chinese Academy of Sciences, Shanghai, China

ARTICLE INFO

Keywords:

Diabetes mellitus
Cognitive impairment
ChemR23
Oxidative stress
NLRP3 inflammasome

ABSTRACT

Diabetes mellitus is associated with cognitive impairment characterized by memory loss and cognitive inflexibility. Recent studies have revealed that ChemR23 is implicated in both diabetes mellitus and Alzheimer's disease. However, the impact of ChemR23 on diabetes-associated cognitive impairment remains elusive. In this study, we explored the longitudinal changes of ChemR23 expression and cognitive function in STZ-induced type 1 diabetic mice and leptin receptor knockout type 2 diabetic mice at different ages. We also treated diabetic mice with ChemR23 agonists RvE1 or chemerin-9 to explore whether ChemR23 activation could alleviate diabetes-associated cognitive impairment. The underlying mechanism was further investigated in diabetic mice with genetic deletion of ChemR23. The results showed that ChemR23 expression was decreased along with aging and the progression of diabetes, suggesting that abnormal ChemR23 signaling may be involved in diabetes-associated cognitive impairment. Administration of RvE1 or chemerin-9 ameliorated oxidative stress and inhibited NLRP3 inflammasome activation through Nrf2/TXNIP pathway, and ultimately alleviated cognitive impairment in diabetic mice. Depletion of ChemR23 in diabetic mice abolished the beneficial effects of RvE1 and chemerin-9, and exacerbated cognitive impairment via increasing oxidative stress and activating NLRP3 inflammasome. Collectively, our data highlight the crucial role of ChemR23 signaling in diabetes-associated cognitive impairment via regulating oxidative stress and NLRP3 inflammasome, and targeting ChemR23 may serve as a promising novel strategy for the treatment of diabetes-associated cognitive impairment.

1. Introduction

Diabetes mellitus (DM) is one of the most prevalent systemic metabolic diseases characterized by hyperglycemia [1]. Clinical and epidemiological studies have demonstrated that diabetic patients have a higher risk of cognitive dysfunction and dementia than non-diabetic individuals [2,3]. Diabetes-associated cognitive impairment (DACI) is manifested as memory loss, cognitive inflexibility, and poor psychomotor performance [4]. The etiology and underlying mechanisms of

DACI development remain unclear.

ChemR23 is widely expressed not only in peripheral monocytes, macrophages, immature dendritic cells, natural killer cells, and adipocytes [5–7], but also in central glial cells and neurons [8–11]. ChemR23 is of interest as it is a seven-pass transmembrane G-protein coupled receptor that binds resolvin E1 (RvE1) in addition to the adipokine chemerin [12]. Resolvins mediate their signaling through multiple receptors, denoted ChemR23, ALX/FPR2, GPR18, and GPR32 [13]. Specifically, ChemR23 acts as a high-affinity bioactive receptor for RvE1

* Corresponding author. Department of Neurology, Shanghai Sixth People's Hospital Affiliated to Shanghai Jiao Tong University School of Medicine, Yishan Road 600, Shanghai, 200233, China.

** Corresponding author. Department of Neurology, Shanghai Sixth People's Hospital Affiliated to Shanghai Jiao Tong University School of Medicine, Yishan Road 600, Shanghai, 200233, China.

E-mail addresses: zhaoyuwu2005@126.com (Y. Zhao), xiuzhewang@hotmail.com (X. Wang).

¹ Contributed equally.

<https://doi.org/10.1016/j.redox.2022.102554>

Received 7 November 2022; Received in revised form 22 November 2022; Accepted 23 November 2022

Available online 24 November 2022

2213-2317/© 2022 The Authors. Published by Elsevier B.V. This is an open access article under the CC BY-NC-ND license (<http://creativecommons.org/licenses/by-nc-nd/4.0/>).

[14]. As endogenous ligands of ChemR23, the biofunctions of RvE1 and chemerin have been implicated in the regulation of inflammation [15–18]. ChemR23 signaling has also been implicated in lipid metabolism and glucose homeostasis in the periphery system [19,20]. For example, ChemR23 expressions were increased in obese and type 2 diabetic *Psammomys obesus*' adipose tissue than in lean normoglycemic *Psammomys obesus*' adipose tissue [21,22]. Similarly, ChemR23 expression was dysregulated in neutrophils in DM, and RvE1 treatment could rescue the dysregulation and improve resolution of inflammation [20]. It has also been shown that chemerin/ChemR23 axis could regulate vascular cell function through NADPH oxidase in obesity [23]. Indeed, as RvE1 and chemerin exert emerging roles in metabolic disorders and inflammation [19,24], the signaling of their common receptor, ChemR23, remains elusive and needs further investigation.

Knowledge about the functions of ChemR23 signaling in the brain is limited. RvE1 and chemerin have shown beneficial effects in models of Alzheimer's disease and stroke [25,26]. Furthermore, RvE1/ChemR23 axis has been implicated in pain disorders that involve mechanisms in the central nervous system [27,28]. Recent evidence has demonstrated that ChemR23 expression is altered in the post-mortem brain of patients with Alzheimer's disease, indicating that ChemR23 might be involved in the regulation of cognitive function [8,29]. However, the role of ChemR23 and its functional mechanism in DACI remain elusive.

In the present study, we investigated the changes of ChemR23 expression in the brain in different diabetic mouse models, and explored the treatment effects of ChemR23 activation by RvE1 and chemerin in DACI. Finally, by using ChemR23 knockout mice, we further tested the underlying mechanisms of ChemR23 signaling in DACI.

2. Materials and methods

2.1. Animals

Male leptin receptor-deficient BKS-Lepr^{em2Cd479}/Gpt mice (db/db) and age-matched C57BLKS/JGpt mice (WT) were obtained from Gem-Pharmatech (Jiangsu, China). ChemR23 knockout mice were generated by Shanghai Model Organisms Center (Shanghai, China). The mice were housed in a specific pathogen-free animal center under controlled temperature (20–25 °C) and light (12 h light/12 h dark) conditions, with water and food available *ad libitum*. All procedures were approved by the ethical committee on animal welfare of Shanghai Sixth People's Hospital Affiliated to Shanghai Jiao Tong University School of Medicine in accordance with the principles outlined in the National Institutes of Health (NIH) Guide for the Care and Use of Laboratory Animals.

Type 1 diabetes (T1DM) was induced as described previously [30, 31]. Briefly, 7-week-old C57BL/6J mice were injected intraperitoneally with a single dose of STZ (150 mg/kg, Sigma-Aldrich) that was freshly dissolved in pH 4.5 citrate buffer. One week after injection, blood glucose levels were measured, and the mice with blood glucose levels that reached 16.7 mmol/L were defined as the T1DM model.

Type 2 diabetes (T2DM) was modeled using db/db mice, characterized by a leptin-receptor defect leading to obesity, hyperglycemia, and hyperinsulinemia by 5–8 weeks of age [32,33].

2.2. Drug administration

RvE1 (Item # 10007848, Cayman Chemical, Ann Arbor, MI) was supplied as a solution in ethanol, which needed to be evaporated under a gentle stream of nitrogen and immediately diluted with sterile phosphate-buffered saline (PBS) before use. Chemerin-9 (C9, Item # 7117, Tocris Bioscience, Bristol, UK), a bioactive cleaved form of full length chemerin corresponding to C-terminal amino acids 148–156, was dissolved in sterile PBS. Mice were treated intraperitoneally with RvE1 (1.5, 3, and 6 µg/kg body weight) or C9 (30 and 60 µg/kg body weight) every other day for four weeks. The control groups were treated with the same volume of PBS as vehicle.

2.3. Experimental design

Part 1: To explore whether ChemR23 was involved in diabetic cognitive dysfunction, the mice were randomly divided into the following groups: For T1DM study (n = 8 mice/group): 20-week-old WT, 20-week-old STZ, 26-week-old WT, and 26-week-old STZ; For T2DM study (n = 12 mice/group): 6-week-old WT, 6-week-old db/db, 18-week-old WT, 18-week-old db/db, 26-week-old WT, and 26-week-old db/db. Morris water maze was performed to assess cognitive function, and then the mice were sacrificed to collect brain samples for qRT-PCR.

Part 2: To investigate whether activation of ChemR23 with RvE1 or C9 could improve cognitive deficits in diabetic mice, the mice were randomly assigned to the following groups: For T1DM study (n = 10 mice/group, all at 26-week-old): WT group, STZ group, STZ + RvE1 group, and STZ + C9 group. For T2DM study (n = 13 mice/group, all at 18-week-old): WT group, db/db (db group), db/db + RvE1 (db + RvE1 group), and db/db + C9 (db + C9 group). After drug administration, Morris water maze was performed to evaluate the effect of RvE1 or C9 treatment on cognitive function. Mice were then sacrificed to obtain brain samples for further studies.

Part 3: To explore whether ChemR23 deficiency could promote the progression of cognitive impairment in diabetes, the mice were divided into the following groups (n = 10/group, all at 20-week-old): STZ group, ChemR23 knockout + STZ (KO STZ group), ChemR23 knockout + STZ + RvE1 (KO STZ + RvE1 group), and ChemR23 knockout + STZ + C9 (KO STZ + C9 group). Cognitive assessment was determined with Morris water maze, after which the mice were sacrificed, and then the brain samples were collected by either snap-frozen by liquid nitrogen and stored at –80 °C, or directly stored in 4% paraformaldehyde for histological analysis.

2.4. Morris water maze test

Morris water maze (MWM) test was performed to investigate the spatial learning and memory as we described previously [34] with minor modifications. In brief, a circular pool (height 50 cm, diameter 120 cm) with a submerged escape platform (10 cm in diameter) 1.0 cm below the water surface was used. The apparatus was filled with tepid water (25 ± 2 °C) and was surrounded by curtains with visual cues of four different shapes and sizes placed in the four quadrants. The orientation navigation test consisted of four trials a day for five consecutive days. For each daily trial, mice were allowed to swim for a maximum trial duration of 60 s and with 10 s on the platform after climbing onto it successfully. If mice failed to reach the platform within 60 s, they were guided to the platform and kept there for 10 s. During each trial, the latency required to reach the platform was measured as the escape latency. A probe trial was performed on the sixth day, during which mice were allowed to navigate freely for 60 s without the platform and the number of platform crossings, the percentage of time spent in the target quadrant, and the average swimming speed were measured automatically using a video tracking system EthoVision® XT 15.

2.5. Histological staining

After behavioral experiments, mice were transcardially perfused with 0.9% saline followed by 4% paraformaldehyde. Paraformaldehyde-fixed brain samples were embedded in paraffin and then sectioned coronally and serially into 4-µm thick slices by a microtome. Slices were stained with hematoxylin and eosin (H&E) using the standard protocol to analyze the neuronal morphology and damage. The immunohistochemical staining was performed according to the protocol of our previous study [35]. Briefly, paraffin slices were deparaffinized, rehydrated, subjected to heat-induced antigen retrieval using a microwave and blocked with 3% donkey serum and 0.3% Triton X-100 in PBS. Subsequently, slices were incubated with 8-hydroxy-2'-deoxyguanosine (8-OHdG) (bs-1278R, 1:200, Bioss, Beijing, China) overnight at 4 °C.

After triple washing in PBS, horseradish peroxidase (HRP)-conjugated immunoglobulin G (IgG) secondary anti-rabbit antibody (GB23303, 1:1000, Servicebio, Wuhan, China) was incubated for 1 h at room temperature. The localization and distribution of immunoreactive positive cells in the brain were visualized under a microscope (IX53, Olympus, Tokyo, Japan).

2.6. Enzyme-linked immunosorbent assay

The levels of interleukin (IL)-1 β (#70-EK201B/3, Multisciences, Hangzhou, China), IL-6 (#70-EK206/3, Multisciences, Hangzhou, China), and IL-18 (#70-EK282/4, Multisciences, Hangzhou, China) in the hippocampus were quantified using enzyme-linked immunosorbent assay (ELISA) kits in accordance with the manufacturer's instructions. Briefly, the brain samples were thawed on ice and homogenized in PBS by an electric tissue grinder. Tissues homogenates were centrifuged at 3000 \times g for 10 min at 4 $^{\circ}$ C, and then the homogenate supernatant was collected and added to the provided ELISA plate. After 90 min incubation, liquid in the plate was drained off and the plate was incubated with biotinylated antibody working solution for 1 h at 37 $^{\circ}$ C. The liquid in the wells was shaken off and incubated with HRP conjugate working solution for 30 min at 37 $^{\circ}$ C followed by five times of washing. Before the stop solution was added, the wells were incubated with a substrate solution for 15 min at 37 $^{\circ}$ C. The optical density was immediately measured at a wavelength of 450 nm.

2.7. Measurement of superoxide dismutase (SOD) activities and malondialdehyde (MDA) levels

The activity of antioxidant marker SOD (#A001-1, Nanjing Jiancheng Bioengineering Institute, Nanjing, China) and the level of oxidative stress marker MDA (#A003-1, Nanjing Jiancheng Bioengineering Institute, Nanjing, China) in the hippocampus were measured using commercially available kits. Briefly, the brain samples were thawed on ice and homogenized in PBS by an electric tissue grinder. Tissues homogenates were centrifuged at 3000 \times g for 10 min at 4 $^{\circ}$ C, and then the homogenate supernatant was collected for the detection of SOD and MDA. All procedures were in accordance with the manufacturer's instructions.

2.8. Transmission electron microscopy

Transmission electron microscope (TEM) was performed to assess the alterations in synaptic density and morphology of the hippocampus. Following transcardial perfusion with PBS containing 4% paraformaldehyde, hippocampal slices were fixed with electron microscopy fixative made of 2.5% glutaraldehyde (pH 7.2) at 4 $^{\circ}$ C for 4 h. After washing with PBS (0.1 M, pH 7.4) thrice, the slices were post-fixed in 1% OsO₄ for 2 h at room temperature. After dehydrating through a graded series of ethanol solutions (30, 50, 70, 80, 95, and 100%) and acetone, the specimens were embedded in resin and polymerized in a 60 $^{\circ}$ C oven for 48 h. Ultrathin sections (70 nm) were cut and stained with uranyl acetate and lead acetate and observed under HT7700 TEM (Hitachi, Tokyo, Japan).

2.9. Western blot analysis

Western blot analysis of protein in the hippocampus was performed as we previously described [36] with minor modifications. Hippocampus tissues were chopped into small pieces and homogenized with RIPA buffer supplemented with protease and phosphatase inhibitors by sonication. The protein concentration was quantified by the BCA kit (Beyotime, Nanjing, China). Different samples with an equal amount of protein were loaded on sodium dodecyl sulfate-polyacrylamide gel electrophoresis (SDS-PAGE) and transferred to polyvinylidene fluoride (PVDF) membranes. Membranes were blocked with 5% non-fat milk or

BSA in TBS-T and then incubated with the following primary antibodies overnight at 4 $^{\circ}$ C, including nuclear factor erythrocyte 2-related factor 2 (Nrf2) (16396-1-AP, 1:1000), apoptosis-associated speck-like protein containing a CARD (ASC) (10500-1-AP, 1:1000) and β -actin (20536-1-AP, 1:1000) all from Proteintech, IL, USA; NADPH quinone oxidoreductase 1 (NQO1) (A0047, 1:1000), heme oxygenase 1 (HO1) (A19062, 1:1000), thioredoxin-interacting protein (TXNIP) (A9342, 1:1000), caspase1 (A0964, 1:1000), synaptophysin (SYN) (A19122, 1:1000) and postsynaptic density protein-95 (PSD95) (A6194, 1:1000) all from Abclonal, Wuhan, China; nucleotide-binding oligomerization domain-like receptor protein 3 (NLRP3) (GB114320, 1:1000, Servicebio, Wuhan, China). After washing with TBS-T for 3 times, the membranes were incubated with horseradish peroxidase (HRP)-conjugated immunoglobulin G (IgG) secondary anti-rabbit antibody (GB23303, 1:1000, Servicebio, Wuhan, China). Immunoblots were visualized using the enhanced chemiluminescence (ECL) kit (Invitrogen, CA, USA). The blots were quantified using ImageJ software to obtain the grayscale value of signals.

2.10. qRT-PCR

The qRT-PCR was performed as we previously described [35]. Total RNAs in the hippocampus were extracted using the RNAeasy™ animal RNA isolation kit with a spin column according to the manufacturer's protocol. Isolated RNAs were reverse-transcribed into cDNA using the PrimeScript™ RT Master Mix (Perfect Real Time) following the standard protocol. The qPCR assay was conducted using TB Green™ Premix Ex Taq™ II (Tli RNaseH Plus) with the Applied Biosystems 7500 Real-Time PCR System (Applied Biosystems, CA, USA). The amplification parameters were 95 $^{\circ}$ C for 30 s, followed by 40 cycles of 95 $^{\circ}$ C for 5 s and 60 $^{\circ}$ C for 34 s, 95 $^{\circ}$ C for 15 s, 60 $^{\circ}$ C for 60 s, and 95 $^{\circ}$ C for 15 s. The gene expression levels were calculated using the 2^{- $\Delta\Delta$ Ct} method. Each sample was analyzed in triplicate, and the relative expression of mRNA was calculated after normalization to β -actin. The relative mRNA expression level in the WT group (target mRNA/ β -actin value) was set to 100%, and the mRNA values in other groups were converted to fold changes after comparison with the control group.

The following PCR primer sequences were used for detecting transcriptions: β -actin, F: 5'-GTGACGTTGACATCCGTAAGA-3', R: 5'-GTAACAGTCCGCCTAGAAGCAC-3'; ChemR23, F: 5'-TACGACGCTTACAACGACTCC-3', R: 5'-TAGGAGACCGAGGAAGCACA-3'.

2.11. RNA sequencing

Three hippocampal samples from each group were randomly selected for RNA Sequencing (RNAseq) experiments. Total RNAs were isolated using Trizol reagent kit (Invitrogen, CA, USA) by following the manufacturer's instructions. RNA quality was measured on an Agilent 2100 Bioanalyzer (Agilent Technologies, CA, USA) and checked using RNase-free agarose gel electrophoresis. And then, the enriched mRNAs were fragmented into short fragments using fragmentation buffer and reversely transcribed into cDNA by using NEBNext Ultra RNA Library Prep Kit for Illumina (NEB #7530, New England Biolabs, MA, USA). The resulting cDNA library was sequenced using Illumina Novaseq6000 by Gene Denovo Biotechnology Co. (Guangzhou, China). Reads obtained from the sequencing machines were further filtered by fastp (version 0.18.0) to get high-quality clean reads. RNA differential expression analysis was performed by DESeq2 software between two different groups. The genes with the parameter of false discovery rate (FDR) below 0.05 and absolute fold change of 1.5 or greater were considered differentially expressed genes (DEGs). The DEGs of each group were subjected to the Gene Ontology (GO) and Kyoto Encyclopedia of Genes and Genomes (KEGG) pathway enrichment functional analysis.

2.12. Statistical analysis

Statistical analysis was performed using GraphPad Prism 7 (GraphPad Software Inc., CA, USA). The data were presented as mean ± standard error of the mean (SEM). Differences between groups were performed using one-way analysis of variance (ANOVA). For the hidden-platform training of the Morris water maze test, the escape latency was analyzed by two-way repeated-measures ANOVA followed by Tukey's post hoc test. Statistical significance was set at $P < 0.05$.

3. Results

3.1. Cognitive dysfunction in diabetic mice correlated with ChemR23 deficiency

To investigate the effect of diabetes on cognitive function, spatial learning and memory performance was assessed via Morris water maze in all age groups of db/db mice and STZ mice. We observed no significant learning impairment in 6-week-old WT and db/db mice, as indicated by a nonsignificant difference in the latency from the 1st to the 5th days. With prolonged diabetes duration, learning capacity was significantly impaired in db/db mice at 18 and 26 weeks of age, as evidenced

by an increase in the escape latency on the 4th and 5th days in comparison to age-matched WT mice (Fig. 1A, D). Twenty-four hours after the last training session, we performed a probe trial, in which the number of times across the retracted platform and the percentage of time spent in the target quadrant were recorded to evaluate memory preservation. There was no significant difference in the time spent in the target quadrant and the number of platform crosses between the 6-week-old WT and db/db mice, while 18- and 26-week-old db/db mice showed difficulties in remembering where the platform was originally placed and spent a significantly shorter time in the target quadrant when compared to age-matched WT mice (Fig. 1B and C). On the other hand, we observed a slight but not significant increase in the escape latency in 20-week-old STZ mice compared to age-matched WT mice, whereas the latency to reach the platform of STZ mice was statistically different compared with WT mice at 26 weeks of age (Fig. 1E, H). Meanwhile, 20-week-old STZ mice exhibited no significant memory impairment, while 26-week-old STZ mice showed significant impairment in memory retention, as evidenced by decreased time in the target quadrant and the number of platform crosses (Fig. 1F and G). Altogether, these results demonstrate that learning and memory performance is impaired along with aging and the progression of diabetes in both db/db and STZ mice.

Given the close association of ChemR23 signaling with diabetes and

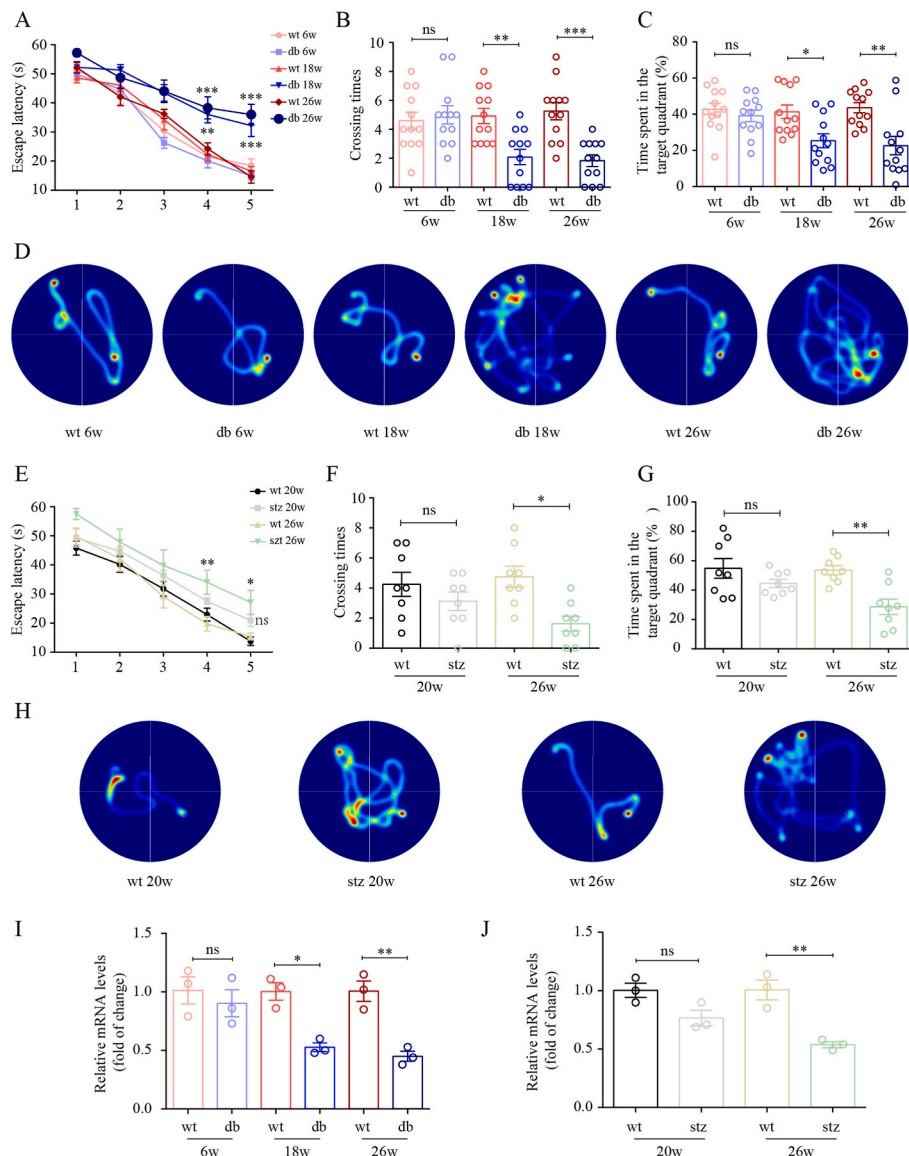


Fig. 1. Age-dependent decline of spatial learning, memory performance and ChemR23 expression in diabetic mice. (A, E) The escape latency of db/db mice and STZ mice in the navigation trials of the hidden platform task. $n = 8-12$ mice/group. (B, F) Frequency of platform crossing of db/db mice and STZ mice in the probe trial. $n = 8-12$ mice/group. (C, G) Percentage of time spent in the target quadrant of db/db mice and STZ mice in the probe trial. $n = 8-12$ mice/group. (D, H) Representative path tracings of db/db mice and STZ mice during the navigation trials. (I, J) qPCR analysis of ChemR23 in the hippocampus of db/db mice and STZ mice at different ages. $n = 3$ mice/group. * $P < 0.05$; ** $P < 0.01$; *** $P < 0.001$.

cognition [29,37], we sought to determine the levels of ChemR23 expression in the hippocampus of two diabetic mouse models. The expression of ChemR23 remained unaffected in both WT and db/db mice at 6 weeks of age. At 18 and 26 weeks of age, db/db mice displayed a significant decrease of ChemR23 expression compared to the age-matched WT mice (Fig. 1I). Moreover, the analysis showed that ChemR23 expression was not significantly different between STZ and WT mice at 20 weeks of age, whereas a dramatic decrease of ChemR23 expression was observed in 26-week-old STZ mice compared with WT mice (Fig. 1J). Taken together, the results above revealed a parallel relationship between cognitive performance and ChemR23 expression, suggesting that cognitive dysfunction in diabetic mice may be related with ChemR23 deficiency.

3.2. Activation of ChemR23 with RvE1 and C9 improved cognitive deficits in diabetic mice

To determine the effect of ChemR23 stimulation on cognitive deficits in diabetic mice, we treated 18-week-old db/db mice and 26-week-old STZ mice with the ChemR23 agonists RvE1 or C9 for 4 weeks. As shown in Figs. S1A–C and Fig. 2A and D, RvE1 dose of 1.5 $\mu\text{g}/\text{kg}$ did not improve learning impairment in db/db mice, while higher doses of RvE1 (3 and 6 $\mu\text{g}/\text{kg}$) significantly decreased the time spent on locating the hidden platform. Furthermore, db/db mice treated with 6 $\mu\text{g}/\text{kg}$ RvE1 exhibited remarkably more preference for the target quadrant and a higher frequency of crossing the platform compared with vehicle-treated db/db mice (Fig. 2B and C). For the treatment study of C9, we observed that the higher dose of C9 (60 $\mu\text{g}/\text{kg}$) but not the lower dose of C9 (30 $\mu\text{g}/\text{kg}$) significantly improved learning and memory performance in db/db mice (Figs. S1A–C). The above results indicated that the higher dose of RvE1 (6 $\mu\text{g}/\text{kg}$) and C9 (60 $\mu\text{g}/\text{kg}$) exerted a better treatment effect. Therefore, 6 $\mu\text{g}/\text{kg}$ of RvE1 and 60 $\mu\text{g}/\text{kg}$ of C9 were selected for further experiments. Similarly, treatment of STZ mice with RvE1 or C9 also significantly decreased the time spent on locating the hidden platform, while it prolonged the staying time in the target quadrant and increased the frequency of platform crossing (Fig. 2E–H). Taken together, these data suggest that the activation of ChemR23 with RvE1 or C9 improves learning and memory capacities in diabetic mice.

3.3. RvE1 and C9 ameliorated neuronal death and synaptic impairment in diabetic mice

The hippocampus is the major region of the brain involved in cognition and memory [37]. As shown by the representative micrographs of H&E staining in the mouse hippocampus (Fig. 3A–D), neuronal degeneration and nuclear shrinkage were observed in db/db and STZ mice, while RvE1 and C9 protected against these neuronal damages. To investigate whether activation of ChemR23 with RvE1 or C9 could improve hippocampal synaptic plasticity in diabetic mice, the alterations in the synaptic structure of hippocampal neurons were studied by TEM. The length of postsynaptic density (PSD) was remarkably reduced in the hippocampus of both db/db and STZ mice, while administration of RvE1 or C9 increased the length of PSD in diabetic mice, which was comparable to WT mice (Fig. 3E–H). Furthermore, we analyzed the expressions of the presynaptic and postsynaptic markers, SYN and PSD95 respectively, in the mice hippocampus. Immunoblotting analysis confirmed that the expressions of SYN and PSD95 were noticeably downregulated in both db/db and STZ mice, and RvE1 or C9 treatment enhanced the expressions of SYN and PSD95 (Fig. 3I–L), which is in line with synapse ultrastructural alterations. Altogether, these results indicate that RvE1 or C9 ameliorates neuronal damage with regard to synaptic integrity and plasticity in diabetic mice.

3.4. RvE1 and C9 attenuated oxidative stress in diabetic mice through Nrf2 pathway

To gain insight into potential mechanisms of diabetic cognitive impairment, the transcriptomic changes in the hippocampus of diabetic mice were analyzed. The KEGG analysis of the overlapped DEGs among db/db vs. WT and STZ vs. WT revealed that oxidative phosphorylation, Alzheimer's disease, Parkinson's disease, and dopaminergic synapse are among the most affected pathways. And it has been reported that impairment of mitochondrial oxidative phosphorylation is associated with oxidative stress, which is closely related to synaptic impairment and cognitive dysfunction [38–40]. We then sought to further explore the alteration of oxidative stress in DACI (Fig. 4A). Among those oxidative stress-related genes, we identified 6 downregulated and 6 upregulated genes. In particular, three genes including Nfe2l2 (encoding gene for Nrf2), Hmox1 (encoding gene for HO1), and NQO1, all of which are known to be involved in anti-oxidative stress processes, showed

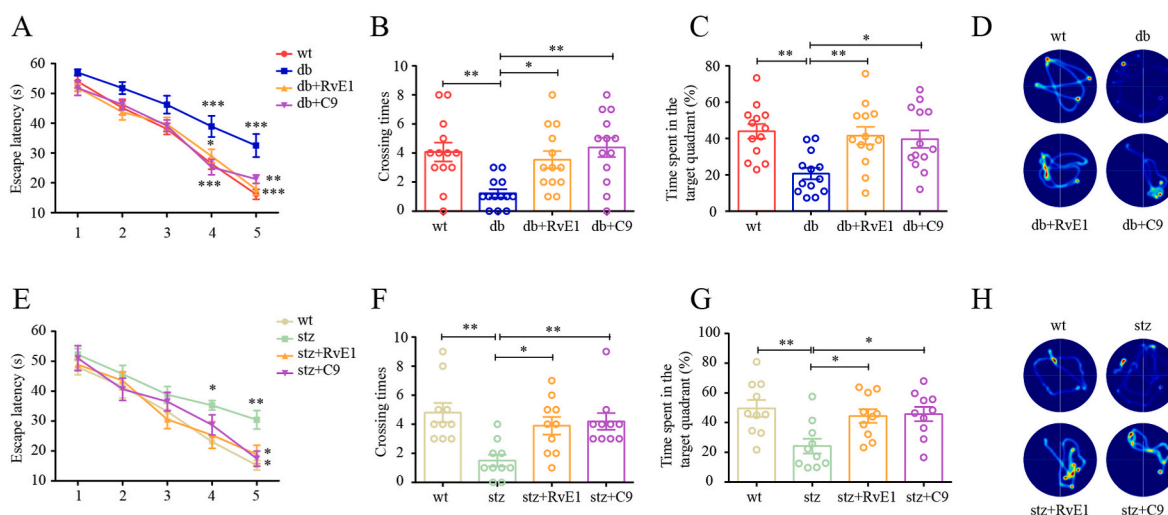


Fig. 2. Activation of ChemR23 with RvE1 or C9 improved cognitive deficits in diabetic mice. (A, E) Escape latency results during platform trials indicated that RvE1 or C9 treatment ameliorated learning and memory dysfunction in db/db mice and STZ mice. $n = 10\text{--}13$ mice/group. (B, F) Frequency of platform crossing of db/db mice and STZ mice after RvE1 or C9 treatment in the probe trial. $n = 10\text{--}13$ mice/group. (C, G) Percentage of time spent in the target quadrant of db/db mice and STZ mice after RvE1 or C9 treatment in the probe trial. $n = 10\text{--}13$ mice/group. (D, H) Representative path tracings of db/db mice and STZ mice after RvE1 or C9 treatment during the navigation trials. $*P < 0.05$; $**P < 0.01$; $***P < 0.001$. C9, chemerin-9.

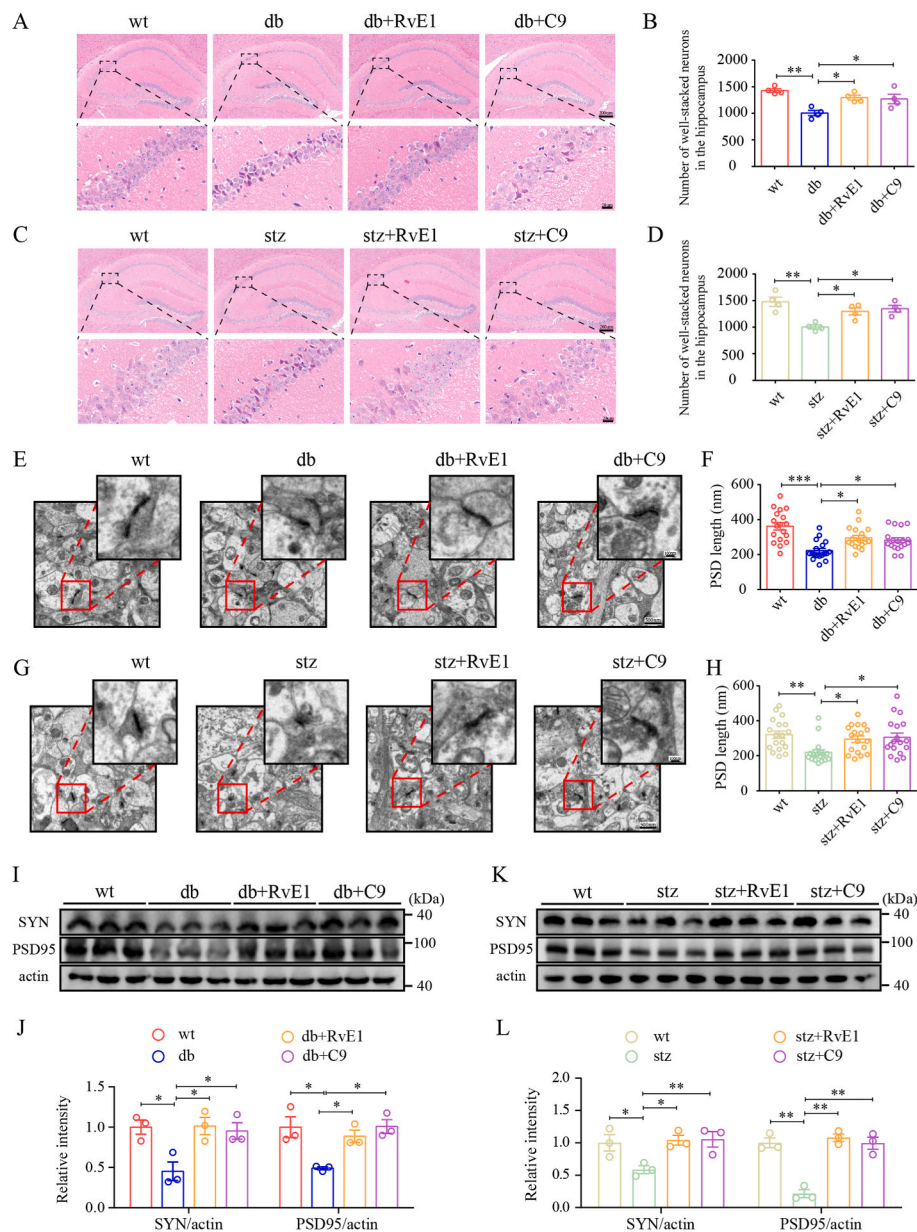


Fig. 3. RvE1 and C9 ameliorated neuronal death and synaptic impairment in diabetic mice. (A, C) Representative H&E staining of neurons in the hippocampus of db/db mice and STZ mice after treatment with RvE1 or C9. (B, D) Number of well-stacked neurons in the hippocampus. n = 4 mice/group. (E, G) Representative images showing the ultrastructure of the synapse in the hippocampus of db/db mice and STZ mice after treatment with RvE1 or C9. (F, H) Quantitative analysis of PSD length. n = 3 mice/group. (I, K) Representative immunoblotting bands of SYN and PSD95 in the hippocampus of db/db mice and STZ mice after treatment with RvE1 or C9. (J, L) Quantitative analysis of SYN/actin and PSD95/actin. n = 3 mice/group. *P < 0.05; **P < 0.01; ***P < 0.001. C9, chemerin-9; H&E, hematoxylin and eosin; SYN, synaptophysin.

significant transcriptional downregulation in diabetes (Fig. 4B).

Therefore, we sought to explore whether activation of ChemR23 ameliorated diabetic cognitive dysfunction through Nrf2 pathway. The immunoblotting studies with hippocampal tissue lysates showed that the expressions of Nrf2, HO1, and NQO1 were observably decreased in db/db and STZ mice, while both RvE1 and C9 significantly reversed these changes (Fig. 4C–F). We then evaluated the activity of antioxidant marker SOD and the level of oxidative stress marker MDA in the hippocampus using commercially available kits. We observed significantly lower activity of SOD and a higher level of MDA in both db/db and STZ mice, whereas either RvE1 or C9 prominently reversed these changes (Fig. 4G–J). Immunohistochemical staining was further performed to determine whether RvE1 and C9 treatment inhibited the production of ROS by measuring 8-OHdG in diabetic mice. We found that the average optical density of 8-OHdG in the hippocampal CA1 was higher in both db/db and STZ mice compared with WT mice. On the other hand, treatment with either RvE1 or C9 observably decreased the levels of 8-OHdG in db/db and STZ mice (Fig. 4K–N). Overall, these results suggest that the activation of ChemR23 by RvE1 and C9 attenuates

oxidative stress through Nrf2 pathway in diabetic mice.

3.5. RvE1 and C9 alleviated the activation of NLRP3 inflammasome in diabetic mice by inhibiting TXNIP

As is known, oxidative stress is able to activate NLRP3 inflammasome, which plays a key role in dementia. It has been reported that TXNIP is prone to bind NLRP3 and leads to its activation under conditions of oxidative stress [41,42]. As expected, the protein levels of TXNIP, NLRP3, ASC, caspase1, and IL-1 β were significantly increased in both db/db and STZ mice compared with WT mice, while administration of RvE1 and C9 decreased the expression of these proteins in the hippocampus of db/db and STZ mice (Fig. 5A–F). Furthermore, ELISA assay was performed to evaluate the levels of pro-inflammatory cytokines (including IL-1 β , IL-6, and IL-18) associated with NLRP3 inflammasome activation. Compared to WT mice, diabetic mice expressed remarkably higher levels of IL-1 β , IL-6, and IL-18 in the hippocampus. On the other hand, db/db and STZ mice receiving either RvE1 or C9 observably rescued these abnormalities (Fig. 5G–L). The results above collectively

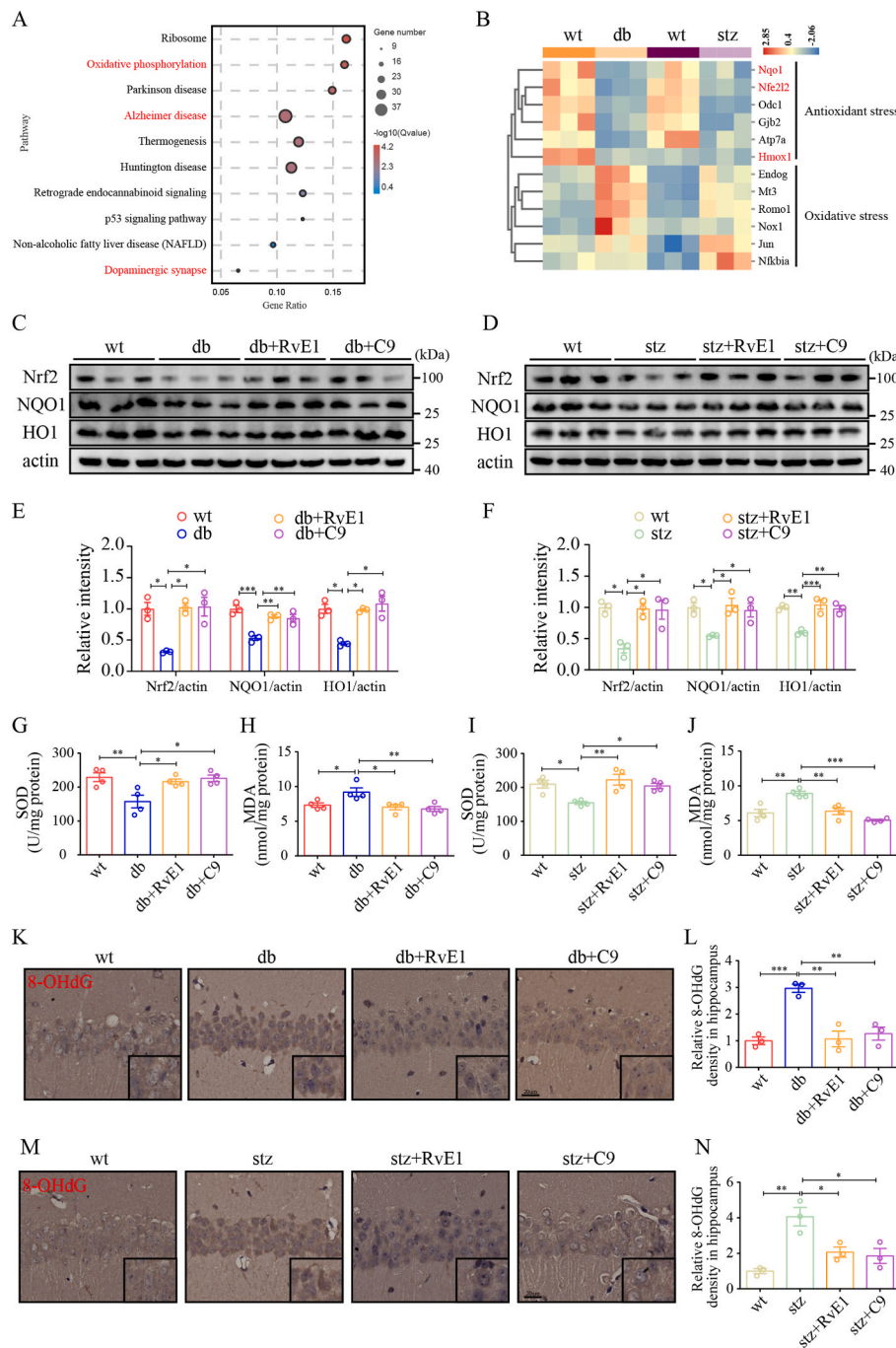


Fig. 4. RvE1 and C9 attenuated oxidative stress through Nrf2 pathway in diabetic mice. (A) Bubble chart showing significant enrichment of DEGs in various pathways. (B) Relative expression levels are shown for genes in oxidative stress-related pathway among db/db vs. WT and STZ vs. WT. n = 3 mice/group. (C, D) Representative immunoblotting bands of Nrf2, NQO1, and HO1 in the hippocampus of db/db mice and STZ mice after treatment with RvE1 or C9. n = 3 mice/group. (E, F) Quantitative analysis of Nrf2/actin, NQO1/actin, and HO1/actin. n = 3 mice/group. (G–J) The activities of SOD and levels of MDA in the hippocampus of db/db mice and STZ mice after treatment with RvE1 or C9 were measured. n = 3 mice/group. (K, M) Representative immunohistochemical staining of 8-OHdG in the hippocampus of db/db mice and STZ mice after treatment with RvE1 or C9. n = 3 mice/group. Scale bar = 20 μm . (L, N) Quantitative analysis of relative 8-OHdG density in the hippocampus. n = 3 mice/group. * $P < 0.05$; ** $P < 0.01$; *** $P < 0.001$. C9, chemerin-9; DEGs, differentially expressed genes.

indicate that the activation of ChemR23 by RvE1 and C9 inhibits NLRP3 inflammasome pathway in diabetic mice by inhibiting TXNIP.

3.6. ChemR23 deficiency exacerbates cognitive deficits and synaptic impairment in diabetic mice

As we observed significant beneficial effects of ChemR23 activation in DACI, we then investigated whether ChemR23 inhibition may exacerbate DACI by knocking out ChemR23 in STZ-induced diabetic mice. Compared with 20-week-old STZ mice, the learning capacity of 20-week-old ChemR23-knockout STZ mice was significantly decreased, as manifested by a prolonged latency to reach the platform, especially on the 5th day (Fig. 6A, D). In the probe trial, 20-week-old ChemR23-knockout STZ mice showed difficulties in remembering where the

platform was originally placed and spent a significantly shorter time in the target quadrant when compared to age-matched STZ mice (Fig. 6B and C). It is worth noting that the learning and memory impairments were not obvious in 20-week-old STZ mice (Fig. 1E–H), but were evident in 20-week-old ChemR23-knockout STZ mice (Fig. 6A–D), suggesting that ChemR23 deficiency promotes the progression of cognitive dysfunction in diabetic mice. Intriguingly, administration of ChemR23-knockout STZ mice with either RvE1 or C9 did not improve learning and memory impairment (Fig. 6A–D), suggesting that the beneficial effect of RvE1 and C9 on cognitive impairment is ChemR23-dependent.

Next, we sought to determine the effect of ChemR23 deficiency on neuronal survival and synaptic plasticity in 20-week-old STZ mice. As shown in Fig. 6E, most of the neurons in the hippocampus of WT STZ mice were intact, with round and full nuclei, while ChemR23-knockout

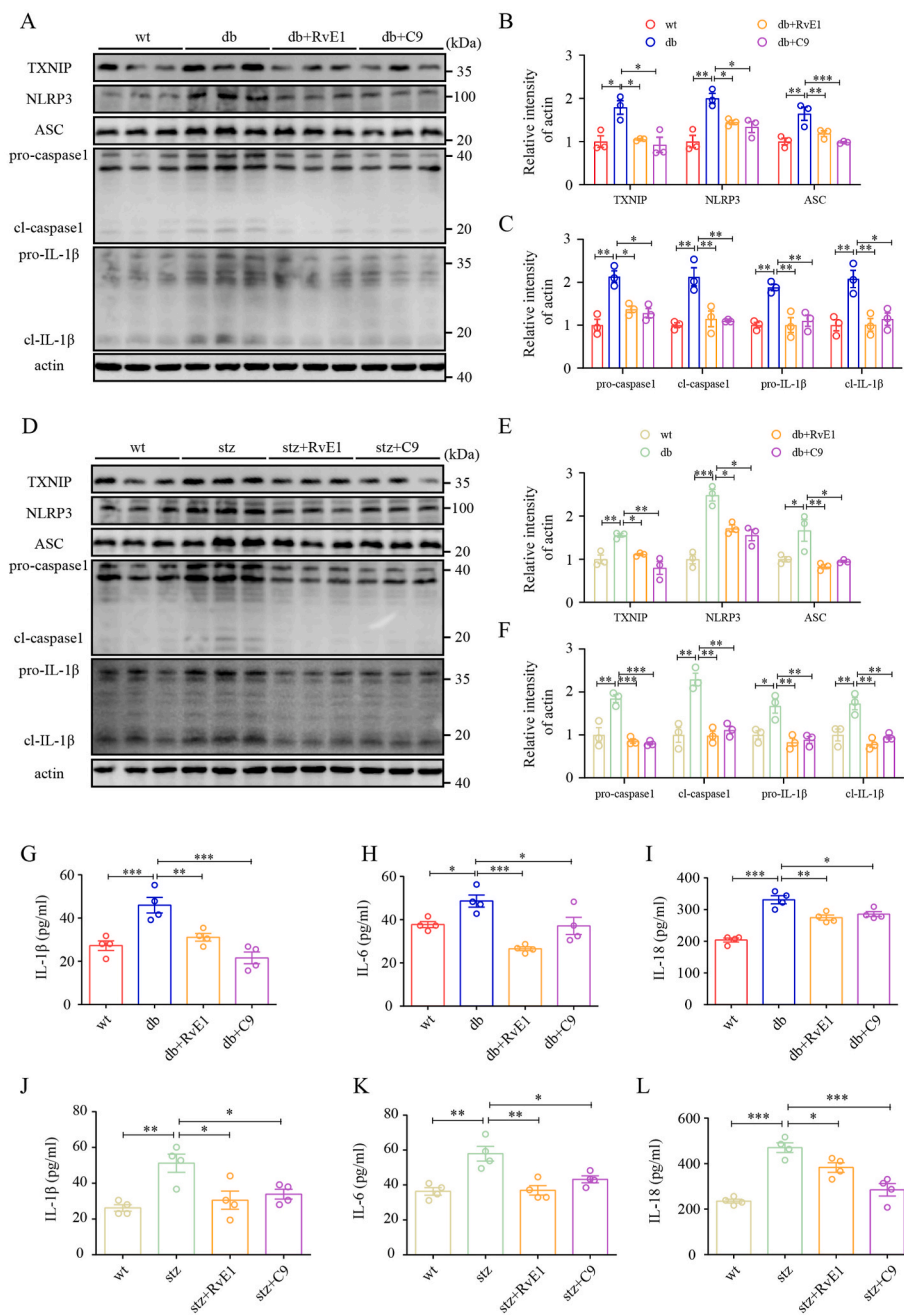


Fig. 5. RvE1 and C9 alleviated NLRP3 inflammasome-mediated neuroinflammation in diabetic mice by inhibiting TXNIP. (A, D) Representative immunoblotting bands of TXNIP, NLRP3, ASC, pro-caspase1, cl-caspase1, pro-IL-1 β , and cl-IL-1 β in the hippocampus of db/db mice and STZ mice after treatment with RvE1 or C9. n = 3 mice/group. (B, C, E, F) Quantitative analysis of TXNIP/actin, NLRP3/actin, ASC/actin, pro-caspase1/actin, cl-caspase1/actin, pro-IL-1 β /actin, and cl-IL-1 β /actin. n = 3 mice/group. (G–L) ELISA was performed to detect the protein levels of IL-1, IL-6, and IL-18 in the hippocampus of db/db mice and STZ mice after treatment with RvE1 or C9. n = 3 mice/group. * P < 0.05; ** P < 0.01; *** P < 0.001. C9, chemerin-9.

STZ mice exhibited abnormal neuronal morphology with shrunken body and dark stained nuclear. Analysis of PSD revealed that the length of the PSD was noticeably shortened in ChemR23-knockout STZ mice in comparison to WT STZ mice (Fig. 6F and G). The immunoblotting analysis also showed significantly lower expressions of SYN and PSD95 in ChemR23-knockout STZ mice as compared with WT STZ mice (Fig. 6H and I). Moreover, RvE1 or C9-treated ChemR23-knockout STZ mice did not restore these changes (Fig. 6E–I), suggesting that the effect of RvE1 and C9 on neuronal damage and synaptic impairment is ChemR23-dependent.

3.7. ChemR23 deficiency aggravates oxidative stress and NLRP3 inflammasome activation in diabetic mice

As mentioned in the earlier results, ChemR23 activation was able to dampen oxidative stress and NLRP3 inflammasome in DACI. Thus,

further experiments were done to explore whether ChemR23 deficiency aggravated DACI by promoting oxidative stress and activating NLRP3 inflammasome. The immunoblotting results demonstrated that the expressions of Nrf2, HO1, and NQO1 were significantly downregulated in ChemR23-knockout STZ mice as compared to WT STZ mice (Fig. 7A and B). We also detected significantly lower activity of SOD and higher levels of MDA in ChemR23-knockout STZ mice (Fig. 7C and D). Moreover, we found that the average optical density of 8-OHdG in the hippocampus was higher in ChemR23-knockout STZ mice compared with WT STZ mice (Fig. 7E and F). Finally, treatment of ChemR23-knockout STZ mice with either RvE1 or C9 could not reverse aggravated oxidative stress (Fig. 7A–F). Then, the effects of ChemR23 knockout on NLRP3 inflammasome pathway were also analyzed. As shown in Fig. 7G–I, the protein levels of TXNIP, NLRP3, ASC, caspase1, and IL-1 β were evidently increased in ChemR23-knockout STZ mice compared with WT STZ mice. And the levels of pro-inflammatory cytokines (including IL-1 β , IL-6, and

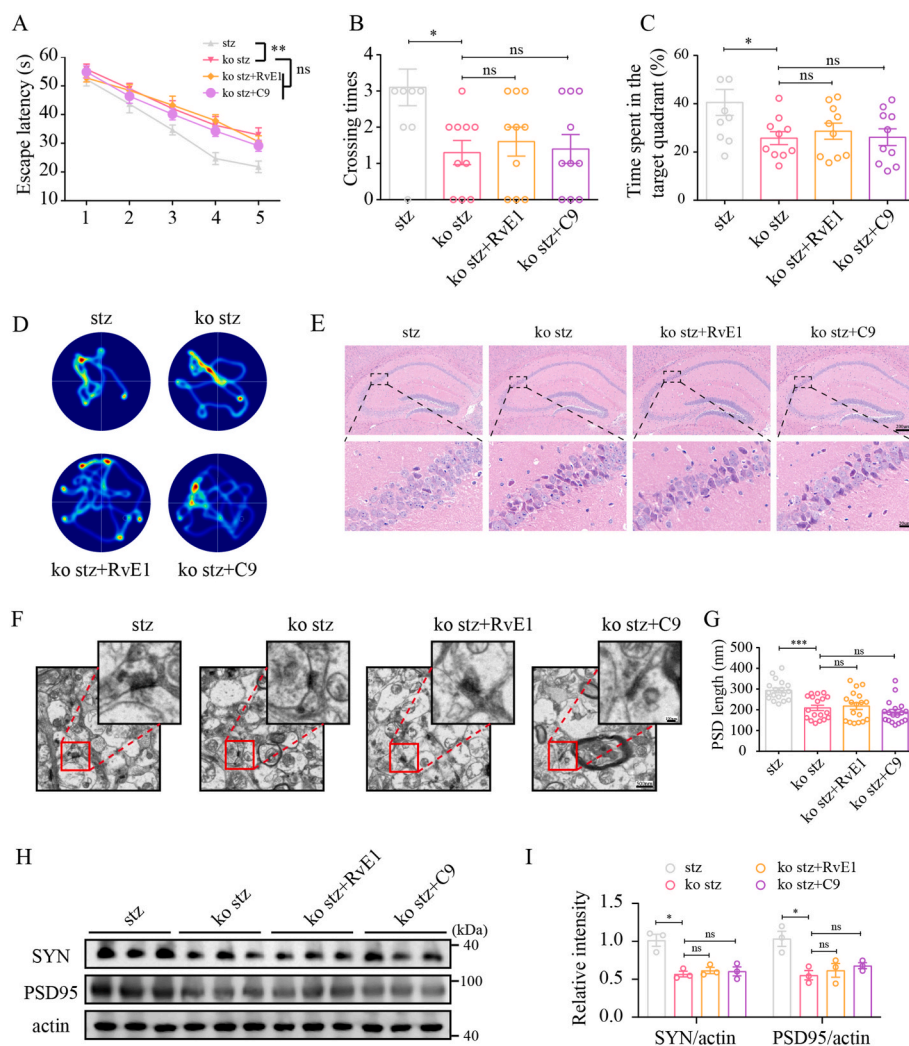


Fig. 6. ChemR23 deficiency exacerbates cognitive deficits and synaptic impairment in diabetic mice. (A) Escape latency results during platform trials indicated that ChemR23 deficiency exacerbated learning and memory dysfunction in STZ-induced diabetic mice. *n* = 10 mice/group. (B) Frequency of platform crossing of ChemR23-knockout STZ mice in the probe trial. *n* = 10 mice/group. (C) Percentage of time spent in the target quadrant of ChemR23-knockout STZ mice in the probe trial. *n* = 10 mice/group. (D) Representative path tracings of ChemR23-knockout STZ mice during the navigation trials. (E) Representative HE staining of neurons in the hippocampus of ChemR23-knockout STZ mice. *n* = 3 mice/group. (F) Representative images showing the ultrastructure of the synapse in the hippocampus of ChemR23-knockout STZ mice. *n* = 3 mice/group. (G) Quantitative analysis of PSD length. *n* = 3 mice/group. (H) Representative immunoblotting bands of SYN and PSD95 in the hippocampus of ChemR23-knockout STZ mice. *n* = 3 mice/group. (I) Quantitative analysis of SYN/actin and PSD95/actin. *n* = 3 mice/group. **P* < 0.05; ***P* < 0.01; ****P* < 0.001. H&E, hematoxylin and eosin; SYN, synaptophysin.

IL-18) were observably increased in the hippocampus of ChemR23-knockout STZ mice (Fig. 7J-L). Furthermore, ChemR23-knockout STZ mice receiving either RvE1 or C9 could not alleviate the activation of NLRP3 inflammasome pathway (Fig. 7G-L). These data collectively indicate that ChemR23 deficiency exacerbates DACI by aggravating oxidative stress and NLRP3 inflammasome activation in diabetic mice.

4. Discussion

Emerging evidence during the last decade has established a close relationship between diabetes and cognitive impairment. Compared with age-matched non-diabetic individuals, patients with either type 1 or type 2 diabetes typically are prone to cognitive decline [43–45]. Cognitive impairment has also been investigated in rodent models of diabetes. For instance, mice rendered diabetic by administration of the pancreatic β-cell toxin STZ, a model of type 1 diabetes, show impaired learning and memory performance in the test of MWM [46]. Similar deficits have also been demonstrated in leptin receptor deficiency db/db mouse, a model of type 2 diabetes [47]. Consistent with previous reports, we found that learning and memory performance was impaired during the progression of diabetes in both db/db and STZ mice. However, there are significant gaps in our knowledge of the mechanisms underlying the relationship between cognitive impairment and diabetes, which limits clinical treatment options.

Recent studies have highlighted the significance of ChemR23 as a therapeutic target involved in diabetes and disorders of the central

nervous system [8,9,29,48]. ChemR23 is a chemoattractant receptor that exerts various biological effects depending on the binding of different ligands [49–51]. Liang et al. reported that chemerin was aggregated in the offspring’s brain of chemerin-challenged diabetic dams and induced macrophage pyroptosis in a ChemR23-dependent manner, thereby leading to cognitive deficits in the offspring [52]. Conversely, chemerin-9 (C9), a cleaved fragment of chemerin, has been reported to ameliorate neuroinflammation and cognitive impairment induced by amyloid β_{1–42} (Aβ_{1–42}) via ChemR23 [53]. Furthermore, RvE1, a derivative of ω-3 fatty acid eicosapentaenoic acid [49,54], interacted with ChemR23 to elicit a significant amelioration of memory loss and neuroinflammation in Ts65Dn mice [55]. In the present study, we provided novel evidence that the decreased expression of ChemR23 in the hippocampus of db/db and STZ mice was paralleled with impaired learning and memory capacities, and showed that chronic activation of this receptor by RvE1 or C9 mitigated cognitive impairment in these diabetic mice. It is widely recognized that hippocampal synaptic plasticity is closely correlated with cognitive function [56]. Studies have also shown a strong relevance between synaptic impairment and cognitive decline in rodent models of diabetes [57–59]. Synaptic activity imposes large energy demands that are met by local adenosine triphosphate (ATP) synthesis through glycolysis and mitochondrial oxidative phosphorylation [60]. Liu Z et al. reported that the expression of energy metabolism-related mitochondrial genes in oxidative phosphorylation is downregulated in db/db mice, which is closely related to synaptic damage and DACI [61]. Moreover, Tian X et al. demonstrated

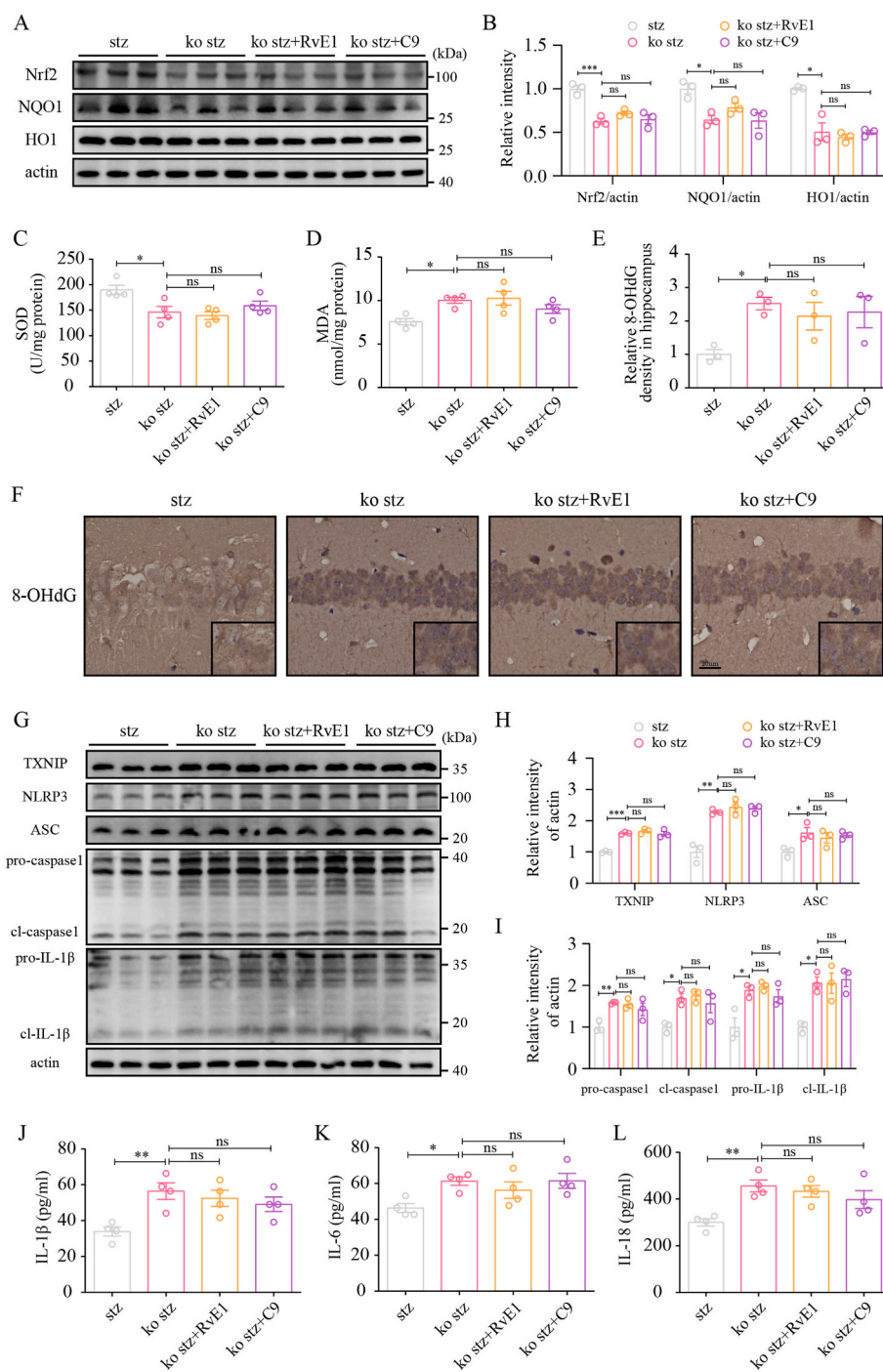


Fig. 7. ChemR23 deficiency abrogates the neuroprotective effects of RvE1 and C9 in diabetic mice (A) Representative immunoblotting bands of Nrf2, NQO1, and HO1 in the hippocampus of ChemR23-knockout STZ mice after treatment with RvE1 or C9. n = 3 mice/group. (B) Quantitative analysis of Nrf2/actin, NQO1/actin, and HO1/actin. n = 3 mice/group. (C, D) The activities of SOD and levels of MDA in the hippocampus of ChemR23-knockout STZ mice after treatment with RvE1 or C9 were measured. n = 3 mice/group. (E) Representative immunohistochemical staining of 8-OHdG in the hippocampus of ChemR23-knockout STZ mice after treatment with RvE1 or C9. n = 3 mice/group. Scale bar = 20 μ m. (F) Quantitative analysis of relative 8-OHdG density in the hippocampus. n = 3 mice/group. (G) Representative immunoblotting bands of TXNIP, NLRP3, ASC, pro-caspase1, cl-caspase1, pro-IL-1 β , and cl-IL-1 β in the hippocampus of ChemR23-knockout STZ mice after treatment with RvE1 or C9. n = 3 mice/group. (H, I) Quantitative analysis of TXNIP/actin, NLRP3/actin, ASC/actin, pro-caspase1/actin, cl-caspase1/actin, pro-IL-1 β /actin, and cl-IL-1 β /actin. n = 3 mice/group. (J–L) ELISA was performed to detect the protein levels of IL-1, IL-6, and IL-18 in the hippocampus of ChemR23-knockout STZ mice after treatment with RvE1 or C9. n = 3 mice/group. * P < 0.05; ** P < 0.01; *** P < 0.001. C9, chemerin-9.

that oxidative stress and neuroinflammation contribute to synaptic impairment and eventually lead to learning and memory deficits in diabetic rats [62]. Consistent with previous studies [47,63], we observed impaired synaptic plasticity in both db/db and STZ mice, as indicated by the shortened length of PSD and lower expression of SYN and PSD95. In addition, we found that activation of ChemR23 by RvE1 or C9 ameliorated while ChemR23-knockout aggravated synaptic damage in diabetic mice, suggesting that ChemR23 deficiency during the progression of diabetes contributes to neural damage and cognitive impairment.

Moreover, we observed that ChemR23-knockout STZ mice developed cognitive impairment earlier and severer than WT-STZ mice, further confirming the significant role of ChemR23 in DACI. In addition to

ChemR23, RvE1 and C9 have been reported to bind and function with other receptors such as BLT1 and CCRL2, respectively [64,65]. To verify that the beneficial effects of RvE1 or C9 were ChemR23-dependent, ChemR23-knockout STZ mice were treated with either RvE1 or C9 and showed no improvement in cognitive impairment. In general, our findings demonstrated that activating of ChemR23 signaling is beneficial in DACI and inhibition of ChemR23 signaling exacerbates DACI in diabetic mice.

The molecular mechanisms of ChemR23 signaling in DACI are of further interest. We sought to investigate the pathogenesis of DACI first. By RNAseq analysis in the hippocampus of diabetic mice, we found that oxidative stress was one of the most affected pathway. Oxidative stress occurs when there is an imbalance between the insufficient generation

of antioxidants and the excessive production of reactive oxygen species (ROS) [66,67]. Considering that the brain function is sensitive to elevated levels of ROS [68–70], sustained oxidative stress is likely among the leading causes of cognitive impairment in diabetes. Previous studies have demonstrated that high glucose concentrations trigger the activation of NADPH oxidase and the generation of ROS [41,71–73]. And a growing body of studies has indicated that excessive oxidative stress contributes to cognitive impairment in rodent models of diabetes [74–76]. In line with previous studies, we observed increased oxidative stress in both db/db and STZ mice, as evidenced by higher levels of oxidative stress markers (MDA and 8-OHdG) and lower activity of antioxidant marker SOD. Growing evidence supported the critical role of mitochondria-derived reactive oxygen species (mtROS) generation in NLRP3 inflammasome activation. Zhou R et al. reported that the loss of mitochondrial membrane potential led to mtROS generation, which further promotes NLRP3 inflammasome activation [77]. The use of a specific mtROS scavenger has been reported to abrogate ROS release and thus inhibit NLRP3 inflammasome activation induced by ethanol, lipopolysaccharide or ATP [78]. Moreover, mtROS overproduction facilitates the interaction between TXNIP and NLRP3, which contributes to the formation and activation of NLRP3 inflammasome [41,79,80]. Once NLRP3 inflammasome is activated, NLRP3 will assemble with ASC to induce the cleavage and activation of caspase-1, which further catalyzes precursors of interleukin-1 β (IL-1 β) and IL-18 into cleaved IL-1 β and mature IL-18, respectively [81,82]. Increasing lines of studies have implicated the activation of NLRP3 inflammasome in DACI, as it has been shown that inhibition of NLRP3 attenuates cognitive impairment in diabetic mice [83–86]. Consistently, in our study, we observed overactivation of NLRP3 inflammasome and increased levels of proinflammatory cytokines (IL-1 β , IL-6, and IL-18) in both db/db and STZ mice. Thus, increased oxidative stress and overactivated NLRP3 inflammasome play crucial roles in DACI, and ChemR23 signaling may interact with these pathways. To confirm this, we demonstrated that chronic activation of ChemR23 by RvE1 or C9 reinstated redox homeostasis and alleviated NLRP3 inflammasome activation, which correlated with improved cognitive performance in MWM test. Moreover, knockout of ChemR23 accelerated oxidative stress and NLRP3 inflammasome activation in diabetic mice, which further confirms that ChemR23 deficiency facilitates these two pathways and eventually leads to DACI.

The link between ChemR23 signaling and oxidative stress/NLRP3 inflammasome is the next question. As a redox-sensitive transcription factor in response to oxidative stress, Nrf2 maintains redox homeostasis via regulating the gene expression of a variety of antioxidant enzymes and phase II detoxification enzymes, including HO1, NQO1, and SOD [87]. It has been reported that Nrf2 activation prevented the onset and progression of DM [88–90]. Importantly, recent studies have shown that Nrf2 activation ameliorates cognitive deficits in both Alzheimer's disease and obese mouse models [91–94], implying that Nrf2 signaling may play an important role against DACI. Nrf2 has also been reported to function as a key gatekeeper of TXNIP transcription, since it keeps the basal expression of TXNIP at a low level and suppresses MondoA-driven induction of TXNIP in diabetes [95]. In our study, we found the expression of Nrf2 was reduced in both db/db and STZ mice. We further showed that RvE1 and C9 treatment significantly enhanced Nrf2 expression in the hippocampus of diabetic mice, accompanied by increased NQO1/HO1 levels and improved cognitive function. On the other hand, ChemR23 knockout led to decreased Nrf2 expression in the hippocampus of diabetic mice, accompanied by decreased NQO1/HO1 levels and exaggerated cognitive impairment. Thus, Nrf2 is possibly the key molecular target of ChemR23 signaling in DACI.

5. Conclusions

In conclusion, our study reveals that ChemR23 deficiency renders synapses susceptible to oxidative stress and NLRP3 inflammasome

activation, and ultimately exacerbates DACI. Moreover, activation of ChemR23 with either RvE1 or C9 ameliorates DACI by inhibiting oxidative stress and NLRP3 inflammasome activation via Nrf2/TXNIP pathway. Altogether, our findings provide evidence that ChemR23 is a potential novel therapeutic target for the treatment of DACI.

Author contributions

X.W. and J.Z. conceived and designed the study. X.W. and Y.Z. (Yuwu Zhao) supervised the research. J.Z. and L.L. performed experiments and analyzed the data. Y.Z. (Yaxuan Zhang), Y.Y., Z.M., and K.L. were involved in animal modeling and data analysis. X.Z., R.N. and H.Z. provided critical suggestions for the study. J.Z. and X.W. draft the manuscript. All of the authors contributed to manuscript writing and approved the final version for publication.

Declaration of competing interest

The authors declare that they have no known competing financial interests or personal relationships that could have appeared to influence the work reported in this paper.

Data availability

Data will be made available on request.

Acknowledgements

This study was supported by research grants from the National Natural Science Foundation of China (Grant No. 81974158 and 82071288).

Appendix A. Supplementary data

Supplementary data to this article can be found online at <https://doi.org/10.1016/j.redox.2022.102554>.

References

- [1] X.L. Wu, M.Z. Deng, Z.J. Gao, Y.Y. Dang, Y.C. Li, C.W. Li, Neferine alleviates memory and cognitive dysfunction in diabetic mice through modulation of the NLRP3 inflammasome pathway and alleviation of endoplasmic-reticulum stress, *Int. Immunopharm.* 84 (2020), 106559.
- [2] R.J. McCrimmon, C.M. Ryan, B.M. Frier, Diabetes and cognitive dysfunction, *Lancet* 379 (9833) (2012) 2291–2299.
- [3] G.J. Biessels, F. Despa, Cognitive decline and dementia in diabetes mellitus: mechanisms and clinical implications, *Nat. Rev. Endocrinol.* 14 (10) (2018) 591–604.
- [4] G.S. Mijnhout, P. Scheltens, M. Diamant, G.J. Biessels, A.M. Wessels, S. Simsek, et al., Diabetic encephalopathy: a concept in need of a definition, *Diabetologia* 49 (6) (2006) 1447–1448.
- [5] A.J. Kennedy, A.P. Davenport, International union of basic and clinical pharmacology CIII: chemerin receptors CMKLR1 (Chemerin1) and GPR1 (Chemerin2) nomenclature, pharmacology, and function, *Pharmacol. Rev.* 70 (1) (2018) 174–196.
- [6] M. Samson, A.L. Edinger, P. Stordeur, J. Rucker, V. Verhasselt, M. Sharron, et al., ChemR23, a putative chemoattractant receptor, is expressed in monocyte-derived dendritic cells and macrophages and is a coreceptor for SIV and some primary HIV-1 strains, *Eur. J. Immunol.* 28 (5) (1998) 1689–1700.
- [7] S. Luangsay, V. Wittamer, B. Bondue, O. De Henaou, L. Rouger, M. Brait, et al., Mouse ChemR23 is expressed in dendritic cell subsets and macrophages, and mediates an anti-inflammatory activity of chemerin in a lung disease model, *J. Immunol.* 183 (10) (2009) 6489–6499.
- [8] X. Wang, M. Zhu, E. Hjorth, V. Cortes-Toro, H. Eyjolfssdottir, C. Graff, et al., Resolution of inflammation is altered in Alzheimer's disease, *Alzheimer's Dementia* :J. Alzheim. Assoc. 11 (1) (2015) 40–50, e41–42.
- [9] Y. Zhang, N. Xu, Y. Ding, Y. Zhang, Q. Li, J. Flores, et al., Chemerin suppresses neuroinflammation and improves neurological recovery via CaMKK2/AMPK/Nrf2 pathway after germinal matrix hemorrhage in neonatal rats, *Brain Behav. Immun.* 70 (2018) 179–193.
- [10] Y. Zhang, N. Xu, Y. Ding, D.M. Doycheva, Y. Zhang, Q. Li, et al., Chemerin reverses neurological impairments and ameliorates neuronal apoptosis through ChemR23/CAMKK2/AMPK pathway in neonatal hypoxic-ischemic encephalopathy, *Cell Death Dis.* 10 (2) (2019) 97.

- [11] H. Zhang, A. Lin, P. Gong, Y. Chen, R.D. Ye, F. Qian, et al., The chemokine-like receptor 1 deficiency improves cognitive deficits of AD mice and attenuates tau hyperphosphorylation via regulating tau seeding, *J. Neurosci. : Off. J. Soc. Neurosci.* 40 (36) (2020) 6991–7007.
- [12] A.E. Al-Shaer, A. Pal, S.R. Shaikh, Resolvin E1-ChemR23 Axis regulates the hepatic metabolic and inflammatory transcriptional landscape in obesity at the whole genome and exon level, *Front. Nutr.* 8 (2021), 799492.
- [13] G. Artiach, M. Carracedo, O. Plunde, C.E. Wheelock, S. Thul, P. Sjoval, et al., Omega-3 polyunsaturated fatty acids decrease aortic valve disease through the resolvin E1 and ChemR23 Axis, *Circulation* 142 (8) (2020) 776–789.
- [14] Z. Miao, M. Schultzberg, X. Wang, Y. Zhao, Role of polyunsaturated fatty acids in ischemic stroke - a perspective of specialized pro-resolving mediators, *Clin. Nutr.* 40 (5) (2021) 2974–2987.
- [15] Z.Z. Xu, L. Zhang, T. Liu, J.Y. Park, T. Berta, R. Yang, et al., Resolvins RvE1 and RvD1 attenuate inflammatory pain via central and peripheral actions, *Nat. Med.* 16 (5) (2010) 592–597, 591pp. following 597.
- [16] J.M. Schwab, N. Chiang, M. Arita, C.N. Serhan, Resolvin E1 and protectin D1 activate inflammation-resolution programmes, *Nature* 447 (7146) (2007) 869–874.
- [17] B. Bondue, V. Wittamer, M. Parmentier, Chemerin and its receptors in leukocyte trafficking, inflammation and metabolism, *Cytokine Growth Factor Rev.* 22 (5–6) (2011) 331–338.
- [18] M.C. Ernst, C.J. Sinal, Chemerin: at the crossroads of inflammation and obesity, *TEM (Trends Endocrinol. Metab.): TEM (Trends Endocrinol. Metab.)* 21 (11) (2010) 660–667.
- [19] G. Helfer, Q.F. Wu, Chemerin: a multifaceted adipokine involved in metabolic disorders, *J. Endocrinol.* 238 (2) (2018) R79–R94.
- [20] M.O. Freire, J. Dalli, C.N. Serhan, T.E. Van Dyke, Neutrophil resolvin E1 receptor expression and function in type 2 diabetes, *J. Immunol.* 198 (2) (2017) 718–728.
- [21] K. Bozaoglu, K. Bolton, J. McMillan, P. Zimmet, J. Jowett, G. Collier, et al., Chemerin is a novel adipokine associated with obesity and metabolic syndrome, *Endocrinology* 148 (10) (2007) 4687–4694.
- [22] S. Perumalsamy, N.A. Aqilah Mohd Zin, R.T. Widodo, W.A. Wan Ahmad, S. Vethakkan, H.Z. Huri, Chemokine like receptor-1 (CMKLR-1) receptor: a potential therapeutic target in management of chemerin induced type 2 diabetes mellitus and cancer, *Curr. Pharmaceut. Des.* 23 (25) (2017) 3689–3698.
- [23] K.B. Neves, A. Nguyen Dinh Cat, R.A. Lopes, F.J. Rios, A. Anagnostopoulou, N. S. Lobato, et al., Chemerin regulates crosstalk between adipocytes and vascular cells through nox, *Hypertension* 66 (3) (2015) 657–666.
- [24] C. Sima, B. Paster, T.E. Van Dyke, Function of pro-resolving lipid mediator resolvin E1 in type 2 diabetes, *Crit. Rev. Immunol.* 38 (5) (2018) 343–365.
- [25] A. Kantarci, N. Aytan, I. Palaska, D. Stephens, L. Crabtree, C. Benincasa, et al., Combined administration of resolvin E1 and lipoxin A4 resolves inflammation in a murine model of Alzheimer's disease, *Exp. Neurol.* 300 (2018) 111–120.
- [26] A. Abareshi, S. Momenabadi, A.A. Vafaei, A.R. Bandegi, A. Vakili, Neuroprotective effects of chemerin on a mouse stroke model: behavioral and molecular dimensions, *Neurochem. Res.* 46 (12) (2021) 3301–3313.
- [27] C.K. Park, Z.Z. Xu, T. Liu, N. Lu, C.N. Serhan, R.R. Ji, Resolvin D2 is a potent endogenous inhibitor for transient receptor potential subtype V1/A1, inflammatory pain, and spinal cord synaptic plasticity in mice: distinct roles of resolvin D1, D2, and E1, *J. Neurosci. : Off. J. Soc. Neurosci.* 31 (50) (2011) 18433–18438.
- [28] H. Suzuki, T. Otsuka, N. Hitora-Imamura, K. Ishimura, H. Fukuda, K. Fujiwara, et al., Resolvin E1 attenuates chronic pain-induced depression-like behavior in mice: possible involvement of chemerin receptor ChemR23, *Biol. Pharm. Bull.* 44 (10) (2021) 1548–1550.
- [29] C. Emre, E. Hjørth, K. Bharani, S. Carroll, A.C. Granholm, M. Schultzberg, Receptors for pro-resolving mediators are increased in Alzheimer's disease brain, *Brain Pathol.* 30 (3) (2020) 614–640.
- [30] K. Wang, F. Song, K. Xu, Z. Liu, S. Han, F. Li, et al., Irisin attenuates neuroinflammation and prevents the memory and cognitive deterioration in streptozotocin-induced diabetic mice, *Mediat. Inflamm.* (2019), 1567179, 2019.
- [31] R. Nie, J. Lu, R. Xu, J. Yang, X. Shen, X. Ouyang, et al., Ipriflavone as a non-steroidal glucocorticoid receptor antagonist ameliorates diabetic cognitive impairment in mice, *Aging Cell* 21 (3) (2022), e13572.
- [32] C.G. Jolival, A. Marquez, D. Quach, M.C. Navarro Diaz, C. Anaya, B. Kifle, et al., Amelioration of both central and peripheral neuropathy in mouse models of type 1 and type 2 diabetes by the neurogenic molecule NSI-189, *Diabetes* 68 (11) (2019) 2143–2154.
- [33] D.R. Garris, Estrogenic stimulation of ovarian follicular maturation in diabetes (db/db) mutant mice: restoration of euglycemia prevents hyperlipidemic cytoatrophy, *Cell Tissue Res.* 318 (2) (2004) 365–373.
- [34] J. Zhang, Y. Zhang, Y. Yuan, L. Liu, Y. Zhao, X. Wang, Gut microbiota alteration is associated with cognitive deficits in genetically diabetic (Db/db) mice during aging, *Front. Aging Neurosci.* 13 (2021), 815562.
- [35] J. Zhang, Y. Zheng, Y. Zhao, Y. Zhang, Y. Liu, F. Ma, et al., Andrographolide ameliorates neuroinflammation in APP/PS1 transgenic mice, *Int. Immunopharm.* 96 (2021), 107808.
- [36] J. Zhang, Y. Liu, Y. Zheng, Y. Luo, Y. Du, Y. Zhao, et al., TREM-2-p38 MAPK signaling regulates neuroinflammation during chronic cerebral hypoperfusion combined with diabetes mellitus, *J. Neuroinflammation* 17 (1) (2020) 2.
- [37] A. Leniz, M. Gonzalez, I. Besne, H. Carr-Ugarte, I. Gomez-Garcia, M.P. Portillo, Role of chemerin in the control of glucose homeostasis, *Mol. Cell. Endocrinol.* 541 (2022), 111504.
- [38] D. Nolfi-Donagan, A. Braganza, S. Shiva, Mitochondrial electron transport chain: oxidative phosphorylation, oxidant production, and methods of measurement, *Redox Biol.* 37 (2020), 101674.
- [39] S. Han, M. Zhang, Y.Y. Jeong, D.J. Margolis, Q. Cai, The role of mitophagy in the regulation of mitochondrial energetic status in neurons, *Autophagy* 17 (12) (2021) 4182–4201.
- [40] V. Rhein, M. Giese, G. Baysang, F. Meier, S. Rao, K.L. Schulz, et al., Ginkgo biloba extract ameliorates oxidative phosphorylation performance and rescues abeta-induced failure, *PLoS One* 5 (8) (2010), e12359.
- [41] R. Zhou, A. Tardivel, B. Thorens, I. Choi, J. Tschopp, Thioredoxin-interacting protein links oxidative stress to inflammasome activation, *Nat. Immunol.* 11 (2) (2010) 136–140.
- [42] M.A. Zaragoza-Campillo, J. Moran, Reactive oxygen species evoked by potassium deprivation and staurosporine inactivate akt and induce the expression of TXNIP in cerebellar granule neurons, *Oxid. Med. Cell. Longev.* (2017), 8930406, 2017.
- [43] A.M. Rawlings, A.R. Sharrett, A.L. Schneider, J. Coresh, M. Albert, D. Couper, et al., Diabetes in midlife and cognitive change over 20 years: a cohort study, *Ann. Intern. Med.* 161 (11) (2014) 785–793.
- [44] C.E. Greenwood, G. Winocur, High-fat diets, insulin resistance and declining cognitive function, *Neurobiol. Aging* 26 (Suppl 1) (2005) 42–45.
- [45] M. Desrocher, J. Rovet, Neurocognitive correlates of type 1 diabetes mellitus in childhood, *Child Neuropsychol. : a journal on normal and abnormal development in childhood and adolescence* 10 (1) (2004) 36–52.
- [46] J. Wang, L. Wang, J. Zhou, A. Qin, Z. Chen, The protective effect of formononetin on cognitive impairment in streptozotocin (STZ)-induced diabetic mice, *Biomed. Pharmacother.* 106 (2018) 1250–1257.
- [47] A.M. Stranahan, T.V. Arumugam, R.G. Cutler, K. Lee, J.M. Egan, M.P. Mattson, Diabetes impairs hippocampal function through glucocorticoid-mediated effects on new and mature neurons, *Nat. Neurosci.* 11 (3) (2008) 309–317.
- [48] S. Deyama, K. Shimoda, H. Suzuki, Y. Ishikawa, K. Ishimura, H. Fukuda, et al., Resolvin E1/E2 ameliorate lipopolysaccharide-induced depression-like behaviors via ChemR23, *Psychopharmacology* 235 (1) (2018) 329–336.
- [49] M. Arita, F. Bianchini, J. Aliberti, A. Sher, N. Chiang, S. Hong, et al., Stereochemical assignment, antiinflammatory properties, and receptor for the omega-3 lipid mediator resolvin E1, *J. Exp. Med.* 201 (5) (2005) 713–722.
- [50] J.L. Cash, R. Hart, A. Russ, J.P. Dixon, W.H. Colledge, J. Doran, et al., Synthetic chemerin-derived peptides suppress inflammation through ChemR23, *J. Exp. Med.* 205 (4) (2008) 767–775.
- [51] V. Wittamer, J.D. Franssen, M. Vulcano, J.F. Mirjolet, E. Le Poul, I. Migeotte, et al., Specific recruitment of antigen-presenting cells by chemerin, a novel processed ligand from human inflammatory fluids, *J. Exp. Med.* 198 (7) (2003) 977–985.
- [52] Z. Liang, L. Han, D. Sun, Y. Chen, Q. Wu, L. Zhang, et al., Chemerin-induced macrophages pyroptosis in fetal brain tissue leads to cognitive disorder in offspring of diabetic dams, *J. Neuroinflammation* 16 (1) (2019) 226.
- [53] Z. Lei, Y. Lu, X. Bai, Z. Jiang, Q. Yu, Chemerin-9 peptide enhances memory and ameliorates abeta1-42-induced object memory impairment in mice, *Biol. Pharm. Bull.* 43 (2) (2020) 272–283.
- [54] C.N. Serhan, N. Chiang, J. Dalli, B.D. Levy, Lipid mediators in the resolution of inflammation, *Cold Spring Harbor Perspect. Biol.* 7 (2) (2014) a016311.
- [55] E.D. Hamlett, E. Hjørth, A. Ledreux, A. Gilmore, M. Schultzberg, A.C. Granholm, RvE1 treatment prevents memory loss and neuroinflammation in the Ts65Dn mouse model of Down syndrome, *Glia* 68 (7) (2020) 1347–1360.
- [56] J.T. Rogers, C.C. Liu, N. Zhao, J. Wang, T. Putzke, L. Yang, et al., Subacute ibuprofen treatment rescues the synaptic and cognitive deficits in advanced-aged mice, *Neurobiol. Aging* 53 (2017) 112–121.
- [57] W.H. Gispen, G.J. Biessels, Cognition and synaptic plasticity in diabetes mellitus, *TINS (Trends Neurosci.)* 23 (11) (2000) 542–549.
- [58] J. Zhou, L. Wang, S. Ling, X. Zhang, Expression changes of growth-associated protein-43 (GAP-43) and mitogen-activated protein kinase phosphatase-1 (MKP-1) and in hippocampus of streptozotocin-induced diabetic cognitive impairment rats, *Exp. Neurol.* 206 (2) (2007) 201–208.
- [59] Z. XiaoMing, Z. Xi, S. Fang, Z. Jilin, Specific changes of somatostatin mRNA expression in the frontal cortex and hippocampus of diabetic rats, *J. Anat.* 204 (Pt 3) (2004) 221–225.
- [60] S. Li, Z.H. Sheng, Energy matters: presynaptic metabolism and the maintenance of synaptic transmission, *Nat. Rev. Neurosci.* 23 (1) (2022) 4–22.
- [61] Z. Liu, X. Dai, H. Zhang, R. Shi, Y. Hui, X. Jin, et al., Gut microbiota mediates intermittent-fasting alleviation of diabetes-induced cognitive impairment, *Nat. Commun.* 11 (1) (2020) 855.
- [62] X. Tian, Y. Liu, G. Ren, L. Yin, X. Liang, T. Geng, et al., Resveratrol limits diabetes-associated cognitive decline in rats by preventing oxidative stress and inflammation and modulating hippocampal structural synaptic plasticity, *Brain Res.* 1650 (2016) 1–9.
- [63] W. Yan, M. Pang, Y. Yu, X. Gou, P. Si, A. Zhatatibai, et al., The neuroprotection of liraglutide on diabetic cognitive deficits is associated with improved hippocampal synapses and inhibited neuronal apoptosis, *Life Sci.* 231 (2019), 116566.
- [64] M. Arita, T. Ohira, Y.P. Sun, S. Elangovan, N. Chiang, C.N. Serhan, Resolvin E1 selectively interacts with leukotriene B4 receptor BLT1 and ChemR23 to regulate inflammation, *J. Immunol.* 178 (6) (2007) 3912–3917.
- [65] T. Yoshimura, J.J. Oppenheim, Chemerin reveals its chimeric nature, *J. Exp. Med.* 205 (10) (2008) 2187–2190.
- [66] S. Salim, Oxidative stress and the central nervous system, *J. Pharmacol. Exp. Therapeut.* 360 (1) (2017) 201–205.
- [67] M. Campolo, G. Casili, M. Lanza, A. Filippone, I. Paterniti, S. Cuzzocrea, et al., Multiple mechanisms of dimethyl fumarate in amyloid beta-induced neurotoxicity in human neuronal cells, *J. Cell Mol. Med.* 22 (2) (2018) 1081–1094.

- [68] H. Yaribeygi, F.R. Farrokhi, A.E. Butler, A. Sahebkar, Insulin resistance: review of the underlying molecular mechanisms, *J. Cell. Physiol.* 234 (6) (2019) 8152–8161.
- [69] Z. Yu, L. Lin, Y. Jiang, I. Chin, X. Wang, X. Li, et al., Recombinant FGF21 protects against blood-brain barrier leakage through Nrf2 upregulation in type 2 diabetes mice, *Mol. Neurobiol.* 56 (4) (2019) 2314–2327.
- [70] Q. Zhao, F. Zhang, Z. Yu, S. Guo, N. Liu, Y. Jiang, et al., HDAC3 inhibition prevents blood-brain barrier permeability through Nrf2 activation in type 2 diabetes male mice, *J. Neuroinflammation* 16 (1) (2019) 103.
- [71] M.R. Dasu, S. Devaraj, I. Jialal, High glucose induces IL-1beta expression in human monocytes: mechanistic insights, *Am. J. Physiol. Endocrinol. Metab.* 293 (1) (2007) E337–E346.
- [72] S.W. Suh, B.S. Shin, H. Ma, M. Van Hoecke, A.M. Brennan, M.A. Yenari, et al., Glucose and NADPH oxidase drive neuronal superoxide formation in stroke, *Ann. Neurol.* 64 (6) (2008) 654–663.
- [73] K. Gokulakrishnan, K.T. Mohanavalli, F. Monickaraj, V. Mohan, M. Balasubramanyam, Subclinical inflammation/oxidation as revealed by altered gene expression profiles in subjects with impaired glucose tolerance and Type 2 diabetes patients, *Mol. Cell. Biochem.* 324 (1–2) (2009) 173–181.
- [74] D.A. Butterfield, F. Di Domenico, E. Barone, Elevated risk of type 2 diabetes for development of Alzheimer disease: a key role for oxidative stress in brain, *Biochim. Biophys. Acta* 1842 (9) (2014) 1693–1706.
- [75] E. Soares, R.D. Prediger, S. Nunes, A.A. Castro, S.D. Viana, C. Lemos, et al., Spatial memory impairments in a prediabetic rat model, *Neuroscience* 250 (2013) 565–577.
- [76] Y.H. Jing, K.H. Chen, P.C. Kuo, C.C. Pao, J.K. Chen, Neurodegeneration in streptozotocin-induced diabetic rats is attenuated by treatment with resveratrol, *Neuroendocrinology* 98 (2) (2013) 116–127.
- [77] R. Zhou, A.S. Yazdi, P. Menu, J. Tschopp, A role for mitochondria in NLRP3 inflammasome activation, *Nature* 469 (7329) (2011) 221–225.
- [78] S. Alfonso-Loeches, J.R. Urena-Peralta, M.J. Morillo-Bargues, J. Oliver-De La Cruz, C. Guerri, Role of mitochondria ROS generation in ethanol-induced NLRP3 inflammasome activation and cell death in astroglial cells, *Front. Cell. Neurosci.* 8 (2014) 216.
- [79] C.Y. Wang, Y. Xu, X. Wang, C. Guo, T. Wang, Z.Y. Wang, DI-3-n-Butylphthalide inhibits NLRP3 inflammasome and mitigates alzheimer's-like pathology via nrf2-TXNIP-TrX Axis, *Antioxidants Redox Signal.* 30 (11) (2019) 1411–1431.
- [80] L. Minutoli, D. Puzzolo, M. Rinaldi, N. Irrera, H. Marini, V. Arcoraci, et al., ROS-mediated NLRP3 inflammasome activation in brain, heart, kidney, and testis ischemia/reperfusion injury, *Oxid. Med. Cell. Longev.* (2016), 2183026, 2016.
- [81] P. Broz, V.M. Dixit, Inflammasomes: mechanism of assembly, regulation and signalling, *Nat. Rev. Immunol.* 16 (7) (2016) 407–420.
- [82] V.A. Rathinam, K.A. Fitzgerald, Inflammasome complexes: emerging mechanisms and effector functions, *Cell* 165 (4) (2016) 792–800.
- [83] Y. Zhai, X. Meng, Y. Luo, Y. Wu, T. Ye, P. Zhou, et al., Notoginsenoside R1 ameliorates diabetic encephalopathy by activating the Nrf2 pathway and inhibiting NLRP3 inflammasome activation, *Oncotarget* 9 (10) (2018) 9344–9363.
- [84] T. Ye, X. Meng, R. Wang, C. Zhang, S. He, G. Sun, et al., Gastrodin alleviates cognitive dysfunction and depressive-like behaviors by inhibiting ER stress and NLRP3 inflammasome activation in db/db mice, *Int. J. Mol. Sci.* 19 (12) (2018).
- [85] Y. Zhai, X. Meng, T. Ye, W. Xie, G. Sun, X. Sun, Inhibiting the NLRP3 inflammasome activation with MCC950 ameliorates diabetic encephalopathy in db/db mice, *Molecules* 23 (3) (2018).
- [86] H.Y. Li, X.C. Wang, Y.M. Xu, N.C. Luo, S. Luo, X.Y. Hao, et al., Berberine improves diabetic encephalopathy through the SIRT1/ER stress pathway in db/db mice, *Rejuvenation Res.* 21 (3) (2018) 200–209.
- [87] H.E. de Vries, M. Witte, D. Hondius, A.J. Rozemuller, B. Drukarch, J. Hoozemans, et al., Nrf2-induced antioxidant protection: a promising target to counteract ROS-mediated damage in neurodegenerative disease? *Free Radical Biol. Med.* 45 (10) (2008) 1375–1383.
- [88] A. Uruno, Y. Furusawa, Y. Yagishita, T. Fukutomi, H. Muramatsu, T. Negishi, et al., The Keap1-Nrf2 system prevents onset of diabetes mellitus, *Mol. Cell Biol.* 33 (15) (2013) 2996–3010.
- [89] Y. Furusawa, A. Uruno, Y. Yagishita, C. Higashi, M. Yamamoto, Nrf2 induces fibroblast growth factor 21 in diabetic mice, *Gene Cell. : devoted to molecular & cellular mechanisms* 19 (12) (2014) 864–878.
- [90] Y. Yagishita, T. Fukutomi, A. Sugawara, H. Kawamura, T. Takahashi, J. Pi, et al., Nrf2 protects pancreatic beta-cells from oxidative and nitrosative stress in diabetic model mice, *Diabetes* 63 (2) (2014) 605–618.
- [91] G. Bahn, J.S. Park, U.J. Yun, Y.J. Lee, Y. Choi, J.S. Park, et al., NRF2/ARE pathway negatively regulates BACE1 expression and ameliorates cognitive deficits in mouse Alzheimer's models, *Proc. Natl. Acad. Sci. U.S.A.* 116 (25) (2019) 12516–12523.
- [92] A. Uruno, D. Matsumaru, R. Ryoke, R. Saito, S. Kadoguchi, D. Saigusa, et al., Nrf2 suppresses oxidative stress and inflammation in app knock-in Alzheimer's disease model mice, *Mol. Cell Biol.* 40 (6) (2020).
- [93] S.A. Lipton, T. Rezaie, A. Nutter, K.M. Lopez, J. Parker, K. Kosaka, et al., Therapeutic advantage of pro-electrophilic drugs to activate the Nrf2/ARE pathway in Alzheimer's disease models, *Cell Death Dis.* 7 (12) (2016) e2499.
- [94] M. Cai, H. Wang, J.J. Li, Y.L. Zhang, L. Xin, F. Li, et al., The signaling mechanisms of hippocampal endoplasmic reticulum stress affecting neuronal plasticity-related protein levels in high fat diet-induced obese rats and the regulation of aerobic exercise, *Brain Behav. Immun.* 57 (2016) 347–359.
- [95] X. He, Q. Ma, Redox regulation by nuclear factor erythroid 2-related factor 2: gatekeeping for the basal and diabetes-induced expression of thioredoxin-interacting protein, *Mol. Pharmacol.* 82 (5) (2012) 887–897.